Secondary Dark Rings of Internal Conical Refraction

Karl F. Warnick and David V. Arnold
Department of Electrical and Computer Engineering
Brigham Young University, 459 Clyde Building, Provo, UT, 84602, USA

This paper treats the phenomenon of internal conical refraction, in which a narrow beam propagating along an optical axis of a biaxial anisotropic medium spreads into a hollow cone. An expression is obtained for the intensity distribution produced by conical refraction that predicts additional fringes concentric to the well–known Poggendorf dark ring for certain propagation distances and beamwidths.

PACS numbers: 42.25.Bs, 42.25.Lc, 78.20.Ci, 78.20.Fm

I. INTRODUCTION

A biaxial anisotropic medium exhibits the phenomenon of internal conical refraction, in which a narrow beam propagating along one of the optical axes of the medium spreads into a hollow cone. Conical refraction was predicted by Hamilton in 1832 and observed shortly thereafter by Lloyd. A dark ring in the center of the circular intensity pattern produced by conical refraction was observed by Poggendorf in 1839 and later explained by Voigt. These historical references and an elementary treatment of conical refraction are found in Born and Wolf [1]. Interest in conical refraction is primarily theoretical, although applications have been suggested [2, 3, 4].

Subsequent to Voigt's work, internal conical refraction has been treated analytically by Portigal and Burstein [5], Lalor [6], Juretschke [7], and Schell and Bloembergen [8]. The latter authors compare experimental and theoretical intensity patterns for internal conical refraction in Aragonite. A recent experimental measurement for conical refraction in KTP is found in Ref. [9].

Related work includes that of Uhlmann [10], who gives a proof of the existence of the dark ring but does not examine the structure of the intensity pattern in detail. Conical refraction in an inhomogeneous, weakly biaxial medium has been considered [11]. Belskii [12] obtains transmission coefficients for a thin biaxial plate along the optical axes, and

Belskii *et al.* [13] discuss the change in astigmatism of a Gaussian beam propagating along an optical axis. Khatkevich [14] shows that a conically refracted beam is not confined to a particular generator of the cone, and plane wave solutions for conical refraction are discussed by Alexandroff [15]. The application of conical refraction in gyrotropic media to beam focusing has been investigated in Refs. [2, 3, 4].

Previous analytical treatments of conical refraction generally amount to a two–dimensional stationary phase evaluation of an inverse Fourier transform integral for field intensity. The wave surface for a biaxial medium consists of an external and an internal sheet which meet in the directions of two optical axes. Near each of the singular points, the wave surface has the shape of a cone. To each wave direction correspond two ray vectors, one due to the external sheet of the wave surface and the other to the internal sheet. The contributions are shifted respectively to the inside and outside of the cone of refraction, so that a dark ring appears in the center of the circular intensity pattern produced by conical refraction [8].

We present a more accurate method of evaluating the integral expression for field intensity due to internal conical refraction. The integration in azimuthal wave vector angle is performed by stationary phase. The remaining transverse integration is then evaluated analytically in terms of special functions. Our results agree with the theoretical and experimental results of Schell and Bloembergen for a 1 cm Aragonite sample, a 34 μm beam waist, and a wavelength of .6328 μm. Schell and Bloembergen also evaluate the field intensity using numerical integration for a crystal length of 10 cm. Their results at this length are qualitatively similar to the 1 cm measurements, with a single dark ring near the center of the circular intensity pattern. For a crystal length of 10 cm, our results indicate further structure in the intensity pattern. Secondary dark rings, or fringes, appear on the inside of the conical intensity pattern.

Apparently, these secondary dark rings have not been predicted or observed for a biaxial, non–optically active medium with real permittivity. The fringes appear only for certain values of beam and material parameters, and no experimental results have been published for measurements in the regime for which the secondary fringes should appear. Measurements by Schell and Bloembergen [16] indicate the appearance of secondary rings for conical refraction by an optically active medium. For a crystal with similar material parameters but neglecting

optical activity, our method gives intensity patterns with qualitative similarity to these experimental results. A series of nulls in the intensity pattern have been predicted for conical refraction in gyrotropic media [2, 3]. We give reasonable values for beam and material parameters for which the secondary rings should be observable, and discuss generally the determination of regimes for which fringes are expected to appear for arbitrary media.

II. PROPAGATION ALONG AN OPTICAL AXIS

To evaluate the electric field intensity due to internal conical refraction, we use the Fourier representation of the tensor Green function for a biaxial, nonmagnetic medium with real, symmetric permittivity tensor. The field can then be obtained from an equivalent current source at the focus of a Gaussian beam by an inverse Fourier transform.

The tensor Green function for a biaxial, nonmagnetic material is [17]

$$G(\mathbf{k},\omega) = \left[k^2(1-\hat{\mathbf{n}}\hat{\mathbf{n}}) - \omega^2\mu\bar{\bar{\epsilon}}\right]^{-1} \tag{1}$$

where ω is the time frequency, $\mathbf{k} = k\hat{\mathbf{n}}$ is the wave vector, μ is the permeability of the medium, and $\bar{\bar{\epsilon}}$ is the real, symmetric permittivity tensor of the medium. The Green function can be conveniently represented by a spectral decomposition [17]

$$G = \sum_{j=1}^{3} \frac{\mathbf{v}_j\mathbf{v}_j}{\omega^2\mu\left(\frac{k^2}{k_j^2}-1\right)} \tag{2}$$

where the polarization vectors $\mathbf{v}_j$ satisty $\left[k^2(1-\hat{\mathbf{n}}\hat{\mathbf{n}}) - \omega^2\mu\bar{\bar{\epsilon}}\right]\mathbf{v}_j = 0$ and are normalized such that

$$\mathbf{v}_j\bar{\bar{\epsilon}}\mathbf{v}_j = 1. \tag{3}$$

The k_j are the corresponding solutions to the Fresnel equation $\det\left[k^2(1-\hat{\mathbf{n}}\hat{\mathbf{n}}) - \omega^2\mu\bar{\bar{\epsilon}}\right] = 0$. One of the k_j is infinite; the associated term of (2) is the nonpropagating part of G.

The wave surface defined by the Fresnel equation consists of two sheets, corresponding to the two nonzero solutions of the Fresnel equation for each wavevector direction $\hat{\mathbf{n}}$. The external and internal sheets of the wave surface meet along the optical axes or binormals. Let (x', y', z') be the principle coordinate system of the permittivity tensor. If the eigenvalues

are ordered so that $\epsilon_1 < \epsilon_2 < \epsilon_3$, then the optical axes lie in the x'-z' plane, at angles

$$\tan\beta = \pm\sqrt{\frac{\epsilon_3(\epsilon_2-\epsilon_1)}{\epsilon_1(\epsilon_3-\epsilon_2)}}. \tag{4}$$

from the z' axis. Near these directions, the wave surface forms a cone. Let x, y, z be the rotated coordinates

$$\begin{aligned} x &= x'\cos\beta - z'\sin\beta \\ y &= y' \\ z &= x'\sin\beta + z'\cos\beta \end{aligned} \tag{5}$$

so that the z axis lies in the direction of one of the optical axes. The geometry is depicted in Fig. 1.

In cylindrical coordinates associated with the rotated coordinate system, the wave surface has an expansion about $k_\rho = 0$ of the form $k_z = T_j$, where [18]

$$T_j = k_2 + A[\cos\phi + (-1)^{j+1}]k_\rho - B_j(\phi)k_\rho^2, \tag{6}$$

$$B_j(\phi) = B[1 + (-1)^j D\cos\phi][1 - (-1)^j E\cos\phi] \tag{7}$$

and $k_2 = \omega\sqrt{\epsilon_2\mu}$. The $j = 1$ term corresponds to the external part of the wave surface and $j = 2$ to the inner part. The constants are

$$\begin{aligned} A &= \frac{1}{2}\sqrt{\frac{(\epsilon_3-\epsilon_2)(\epsilon_2-\epsilon_1)}{\epsilon_1\epsilon_3}} \\ B &= \frac{(\epsilon_3+\epsilon_2)(\epsilon_2+\epsilon_1)}{8\epsilon_1\epsilon_3 k_2} \\ D &= \frac{\epsilon_3-\epsilon_2}{\epsilon_3+\epsilon_2} \\ E &= \frac{\epsilon_2-\epsilon_1}{\epsilon_2+\epsilon_1}. \end{aligned}$$

The apex angle of the cone of refraction is $2A$.

Neglecting the nonpropagating term, the tensor Green function for small k_ρ is

$$G = \sum_{j=1}^{2} \frac{\epsilon_2 \mathbf{v}_j \mathbf{v}_j}{k_z^2 - T_j^2} \tag{8}$$

where the $\mathbf{v}_j$ are in the principle coordinate system. The polarization vectors $\mathbf{v}_j$ can be found using the geometric relationship between the electric displacement vector $\mathbf{D}$ and the wave

and ray vectors. The vectors $\mathbf{D}_j$ corresponding to the $\mathbf{v}_j$ either lie in the plane containing the wave vector and the ray vector or are perpendicular to it. For $\mathbf{k}$ along the z axis and ray vectors lying on the cone of refraction,

$$\begin{aligned}\mathbf{D}_1 &= \hat{\mathbf{x}}\cos\frac{\phi}{2} + \hat{\mathbf{y}}\sin\frac{\phi}{2} \\ \mathbf{D}_2 &= -\hat{\mathbf{x}}\sin\frac{\phi}{2} + \hat{\mathbf{y}}\cos\frac{\phi}{2}.\end{aligned}$$

The $\mathbf{v}_j$ are proportional to $\bar{\bar{\epsilon}}^{-1}\mathbf{D}_j$, so that

$$\mathbf{v}_1 = N\left(\hat{\mathbf{x}}'\epsilon_1^{-1}\cos\beta\cos\frac{\phi}{2} + \hat{\mathbf{y}}'\epsilon_2^{-1}\sin\frac{\phi}{2} - \hat{\mathbf{z}}'\epsilon_3^{-1}\sin\beta\cos\frac{\phi}{2}\right) \tag{9}$$

with the normalization

$$N = \left(\epsilon_1^{-1}\cos^2\beta\cos^2\frac{\phi}{2} + \epsilon_2^{-1}\sin^2\frac{\phi}{2} + \epsilon_3^{-1}\sin^2\beta\cos^2\frac{\phi}{2}\right)^{-\frac{1}{2}} \tag{10}$$

The eigenvector $\mathbf{v}_2$ is $\mathbf{v}_1(\phi+\pi)$.

We place an equivalent gaussian current $\mathbf{J} = J_0\hat{\mathbf{p}}$ at the waist of the beam, where

$$J_0 = \frac{2E_0}{\eta_2}e^{-\rho^2/w_0^2}\,\delta(z) \tag{11}$$

and $\hat{\mathbf{p}}$ specifies the polarization of the beam in the principle coordinate system. w_0 specifies the waist size of the beam at its focus and η_2 is the wave impedance $\sqrt{\mu/\epsilon_2}$. The beam is assumed to be focused at the incident face of the medium. The electric field is then

$$\mathbf{E} = \frac{i\omega\mu}{8\pi^3}\int d\mathbf{k}\, e^{i\mathbf{k}\cdot\mathbf{r}}G(\mathbf{k})J_0(k_\rho)\hat{\mathbf{p}} \tag{12}$$

where $J_0(k_\rho) = (2E_0/\eta_2)\pi w_0^2 e^{-w_0^2 k_\rho/4}$. Integrating k_z by a contour closing in the upper half plane yields

$$\mathbf{E} = -\frac{k_2}{8\pi^2\omega}\int k_\rho\, dk_\rho\, d\phi e^{ik_\rho(x\cos\phi + y\sin\phi)}J_0(k_\rho)\sum_j \mathbf{v}_j(\mathbf{v}_j\cdot\hat{\mathbf{p}})e^{iT_j z} \tag{13}$$

where we assume $z > 0$. The leading order phase as a function of ϕ for both the external and internal terms is

$$g(\phi) = (x + Az)\cos\phi + y\sin\phi. \tag{14}$$

The phase is stationary at two angles; for each of the two terms one of the stationary points is nonphysical. The causal stationary points are

$$\cos\phi_j = (-1)^j\frac{(x+Az)}{\sqrt{(x+Az)^2 + y^2}} \tag{15}$$

where the signs are chosen by noting that ϕ_j specifies the angle of the point on the external or internal sheet of the wave surface at which the surface normal is in the direction of the ray to the point (x, y, z). Integrating (13) by the method of stationary phase gives

$$\mathbf{E} = -\frac{k_2 w_0^2}{4\pi\omega\eta_2} e^{ik_2 z} \sum_j \sigma_j \mathbf{v}_j (\mathbf{v}_j \cdot \hat{\mathbf{p}}) \int k_\rho \, dk_\rho \left(\frac{2\pi}{k_\rho |g_j''|} \right)^{1/2} e^{ik_\rho b_j - k_\rho^2 a_j} \tag{16}$$

where

$$\sigma_j = \exp\left[(-1)^{j+1}\frac{\pi}{4}\right], \tag{17}$$

$$g_j(\phi_j) = (-1)^{j+1}\sqrt{(x+Az)^2+y^2} = -g_j''(\phi_j), \tag{18}$$

$$a_j = \frac{w_0^2}{4} + iB_j(\phi_j)z, \tag{19}$$

$$b_j = (-1)^{j+1}[Az - \sqrt{(x+Az)^2+y^2}], \tag{20}$$

and the $\mathbf{v}_j$ are evaluated at the stationary point ϕ_j. The large parameter is $k_\rho\sqrt{(x+Az)^2+y^2}$, so that the stationary phase condition becomes invalid as k_ρ grows small. Due to the additional factor of k_ρ in the integrand, however, the complete integrand of (16) is quite accurate for all values of k_ρ, as verified by the numerical techniques discussed below.

The remaining k_ρ integration yields

$$\mathbf{E} = -\frac{\epsilon_2 w_0^2 e^{ik_2 z}}{4\sqrt{\pi}[(x+Az)^2+y^2]^{1/4} a_1^{3/4}} \mathbf{v}_1(\phi_1)[\mathbf{v}_1(\phi_1)\cdot\hat{\mathbf{p}}]\, F(a_1, b_1) \tag{21}$$

where

$$F(a,b) = e^{-b^2/(4a)}\left[\Gamma(1/2)\Gamma(5/4)L_{1/4}^{-1/2}\left(\frac{b^2}{4a}\right) - \frac{b}{\sqrt{a}}\Gamma(3/2)\Gamma(3/4)L_{-1/4}^{1/2}\left(\frac{b^2}{4a}\right)\right] \tag{22}$$

and $L_q^p(x)$ is the associated Laguerre function. The internal and external terms combine since they differ only by the sign of b_j and the phase σ_j. For large z, a_1 is approximately $iB_1 z$, so that the asymptotic dependence of E is $z^{\,5/4}$, which matches the result reported by Moskvin *et al.* [18] for the field due to a point source in directions lying on the cone of internal conic refraction.

For fixed z, the leading behavior of (21) at large distances from the cone of refraction in the x-y plane is the gaussian term $\exp[-b_1^2/(4a_1)]$, where b_1 is the distance from the circular section of the cone with radius Az and center at $(-Az, 0, z)$ as shown in Fig. 2. The polarization term $\mathbf{v}_1(\phi_1)[\mathbf{v}_1(\phi_1)\cdot\hat{\mathbf{p}}]$ modulates the intensity pattern as a function of angle around the cone in the x-y plane, as exhibited by Fig. 3 of Ref. [8].

Expression (21) is singular at the center of the cone of refraction, since the stationary phase condition used in obtaining (16) is invalid at that point. For points away from the center of the cone, (21) is quite accurate, as has been verified by numerical integration of (13). The k_ρ integral in (13) can be evaluated in terms of associated Laguerre functions or hypergeometric functions. The ϕ integration is then performed numerically. Numerical results obtained in this manner for Aragonite ($n_x = 1.530$, $n_y = 1.680$, $n_z = 1.685$ [8]), $z = 10$ cm, beam waist 34 μm, vacuum wavelength .6328 μm, and incident polarization in the x direction differ from the approximate expression (21) by less than two percent over most of the intensity pattern, as shown in Fig. 3.

The feature of (21) that is of main interest here is the oscillatory behavior of F as b_1 varies. This includes the the well-known dark ring that appears slightly inside the cone of internal refraction, but for certain values of the beam waist, propagation distance, and the parameters of the medium, additional fringes appear on the inside of the cone. This behavior is apparently not detected by other theoretical treatments of internal conic refraction [4, 8, 10, 12, 14] for biaxial media with real permittivities, nor have experimental results for conical refraction been published with beam and material parameters for which the secondary dark rings are expected to appear.

Figure 4 shows the magnitude of $F(1 + iy, x)$. For $y > 3$, fringes begin to appear in the interior of the cone. Thus, the structure of the intensity pattern of internal conical refraction depends on

$$\mathrm{Arg}\{a_1\} = \tan^{-1}\frac{4Bz}{w_0^2} \tag{23}$$

where we have assumed that $B_1 \simeq B$, which is true for most materials with relatively small anisotropy. From Fig. 4, the first fringe begins to appear for $\mathrm{Arg}\{a_1\} \approx 1.3$. As $\mathrm{Arg}\{a_1\}$ increases, additional fringes appear. For fixed sample length and wavelength, in order to observe fringes the beam width must be such that $\mathrm{Arg}\{a_1\} \geq 1.25$ and the distance of the fringes from the cone of refraction is smaller than the radius Az of the cone. The width of the intensity pattern is on the order of

$$W = \sqrt{w_0^2 + 16B^2\frac{z^2}{w_0^2}}. \tag{24}$$

If W is significantly larger than the radius Az, the circular intensity pattern of conical

refraction extends to the center of the cone and fringes are obscured. These considerations allow determination of the regimes for which secondary dark rings are expected.

Secondary dark rings should appear in the intensity pattern for an Aragonite crystal of length 1 cm, a wavelength of .6328 μm, and a beam waist size of 18 μm, as shown in Fig. 5. For a 10 cm crystal length and a beam waist of 34 μm, our theory also predicts fringing in the intensity pattern (Fig. 6). This does not match the numerical results of Schell and Bloembergen (Fig. 7c of Ref. [8]). Although the shift of the dark ring's minimum towards the interior of the cone and the larger amplitude of the inner peak agree qualitatively, the intensity pattern obtained by Schell and Bloembergen exhibits no additional fringing.

Although the fringes appear on both sides of the primary dark ring when the external and internal contributions to the field are taken separately, the relative phase is such that the total field exhibits fringing only on the interior of the cone of refraction.

III. CONCLUSION

The intensity pattern due to internal conical refraction of a narrow beam by a biaxial medium apparently has a more complicated structure than previously thought, since our theory predicts additional dark rings on the interior of the cone for certain values of the material parameters, beam waist size, wavelength, and propagation distance. We are unable to locate in the literature measurements of the intensity pattern for beam and material parameters for which secondary dark rings would be expected to appear. It seems desirable to further explore conical refraction experimentally. We have given a reasonable sample size and beamwidth for Aragonite at which the fringes should appear and indicated generally how beam and material parameters relate to the appearance of fringing.

An extension of this work would be to determine the relationship between the secondary fringes predicted by our theory and those that appear in the intensity pattern for an optically active medium as reported in Ref. [16].

ACKNOWLEDGEMENTS

This material is based in part upon work supported under a National Science Foundation Graduate Fellowship to KFW.

REFERENCES

[1] M. Born and E. Wolf, *Principles of Optics* (Pergamon, Oxford, 1980).

[2] Y. A. Brodskii, I. G. Kondratev, and M. A. Miller, Radiophys. Quant. Elect. **12**, 1047 (1969).

[3] Y. A. Brodskii, I. G. Kondratev, and M. A. Miller, Radiophys. Quant. Elect. **15**, 447 (1972).

[4] A. M. Goncharenko *et al.*, Opt. Spectrosc. **78**, 787 (1995).

[5] D. L. Portigal and E. Burstein, J. Opt. Soc. Am. **59**, 1567 (1969).

[6] E. Lalor, J. Math. Phys. **13**, 449 (1972).

[7] H. Juretschke, *Crystal Physics: Macroscopic Physics of Anisotropic Solids* (Benjamin, New York, 1974).

[8] A. J. Schell and N. Bloembergen, J. Opt. Soc. Am. **68**, 1093 (1978).

[9] J. P. Féve, B. Boulanger, and G. Marnier, Opt. Commun. **105**, 243 (1994).

[10] G. A. Uhlmann, Comm. Pure Appl. Math. **25**, 69 (1982).

[11] O. N. Naida, Sov. Phys.–JETP **50**, 239 (1979).

[12] A. M. Belskii, Opt. Spectrosc. **55**, 776 (1983).

[13] A. M. Belskii and A. P. Khapalyuk, Opt. Spectrosc. **44**, 312 (1978).

[14] A. G. Khatkevich, Opt. Spectrosc. **46**, 282 (1979).

[15] V. N. Alexandroff, J. Optics **15**, 219 (1984).

[16] A. J. Schell and N. Bloembergen, J. Opt. Soc. Am. **68**, 1098 (1978).

[17] M. Lax and D. F. Nelson, Phys. Rev. B **4**, 3694 (1971).

[18] D. N. Moskvin, V. P. Romanov, and A. Y. Val'kov, Phys. Rev. E **48**, 1436 (1993).

FIGURE CAPTIONS

FIG. 1. Geometry of conic refraction. The z direction is an optical axis. Normals to the wave surface at the singular point generate the cone of refraction.

FIG. 2. A circular cross section of the cone of refraction. b_1 is the distance from (x, y, z) to the cone in the x-y plane.

FIG. 3. Magnitude of E/E_0 for Aragonite, $z = 10$ cm, beam waist 34 μm, and wavelength .6328 μm. Solid line is computed numerically; dotted line is the stationary phase approximation. On the same scale the percentage error is shown as a dashed line. Incident polarization is in the x direction. The cone of refraction intersects the x axis at $x = -3.5$ mm.

FIG. 4. Magnitude of $F(1 + iy, x)$. The local minimum along the x axis produces the dark ring in the intensity pattern of conical refraction; $x > 0$ corresponds to the interior of the cone.

FIG. 5. Same as Fig. 3, except that $z = 1$ cm and $w_0 = 18$ μm. The singularity of (21) at the center of the cone of refraction appears at $x = -.175$ mm.

FIG. 6. Same as Fig. 3, except that dashed lines are magnitudes of the internal and external contributions taken separately and the solid line is total intensity as given by Eq. (21).

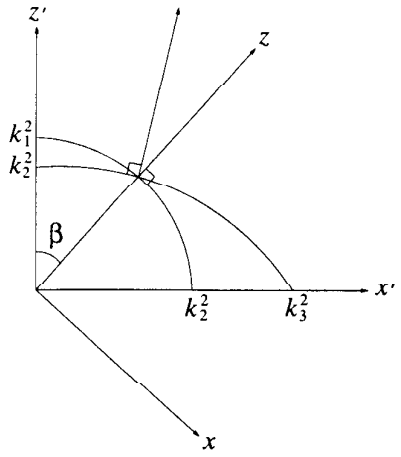

FIG. 1.

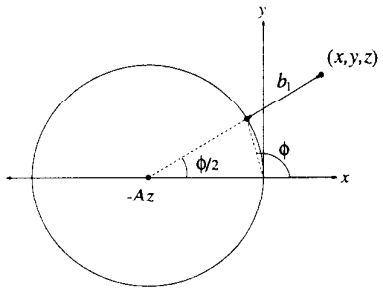

FIG. 2.

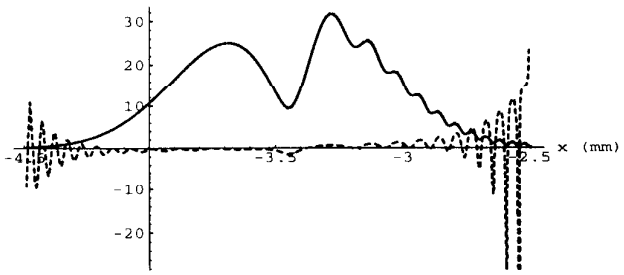

FIG. 3.

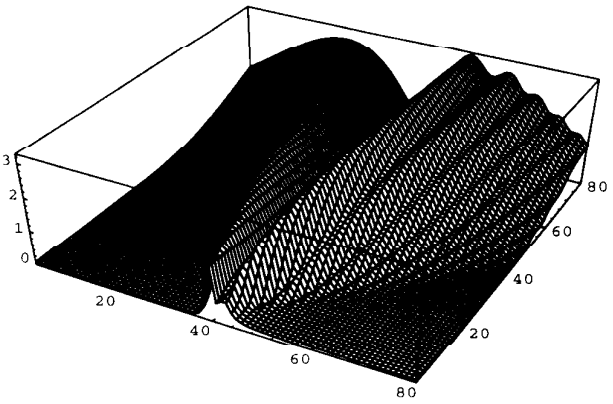

FIG. 4.

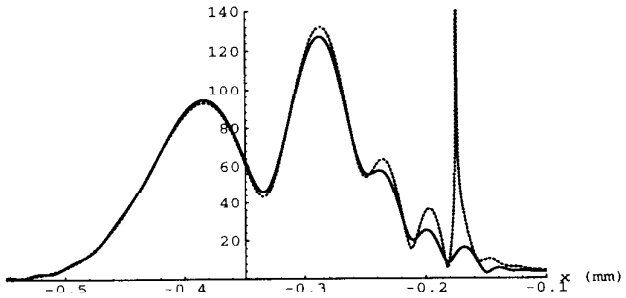

FIG. 5.

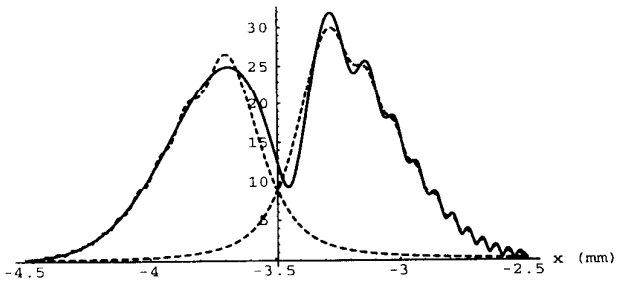

FIG. 6.